Band bendings, band offsets, and interface instabilities in p^+-GaAs/n^--ZnSe heterojunctions

D. J. Olego
Philips Laboratories, North American Philips Corporation, 345 Scarborough Road, Briarcliff Manor, New York 10510
(Received 30 January 1989)

The band bendings at the heterojunction interface between heavily doped p-type GaAs substrates and lightly doped n-type ZnSe epitaxial layers were studied with electric-field-induced Raman scattering by longitudinal-optical phonons. Molecular-beam epitaxy was used to deposit the ZnSe layers. The band bendings were determined as functions of sample temperature and time elapsed after formation of the junctions for different thicknesses of nominally conductive and nonconductive ZnSe layers. These determinations yielded insight into the ability of the Fermi level to respond at the interface according to various heterostructure parameters and external perturbations and allowed an estimation of the band offsets. A temporal evolution of the band bendings with time constants on the order of several days after formation of the junctions was detected. This effect is attributed to instabilities of the GaAs/ZnSe interface due to atomic exchange.

I. INTRODUCTION

There is a renewed interest in the basic properties and potential applications of semiconductor heterostructures made of III-V and II-VI compound semiconductor materials. This interest stems, in part, from the advances in epitaxial-growth techniques, which have yielded the capability of obtaining high-quality II-VI layers on III-V substrates with abrupt interfaces on atomic scales. The GaAs/ZnSe system is one of such III-V–II-VI systems that have recently attracted considerable attention. It has been shown that ZnSe layers can modify the optoelectronic properties of the GaAs surface,[1,2] and can either improve the performance or be instrumental in the operation of GaAs devices.[3–5] Novel GaAs/ZnSe tunneling structures have also been proposed.[6] Their characteristics have been computed and compared with those of GaAs/$Ga_{1-x}Al_xAs$ devices. Optical nonlinearities and integrated optical waveguiding in the visible are also expected to be achievable with GaAs/ZnSe heterostructures. The exploitation and further development of these ideas and technologies require a broad knowledge of the physics and behavior of the interfaces between GaAs and ZnSe. With this in mind, we have undertaken an investigation of band bending effects in p^+-GaAs/n^--ZnSe anisotype heterojunctions. They were formed by growing, with molecular-beam-epitaxy, lightly doped n-type ZnSe layers on heavily doped p-type GaAs substrates.[7] We have applied Raman spectroscopy in this study and the band bendings were established from the intensities of the electric-field-induced scattering by longitudinal-optical phonons. Optical techniques, in general, and Raman scattering, in particular, are well suited to study the optoelectronic properties of ZnSe/GaAs interfaces. This is because the critical layer thickness h_c for the generation of misfit dislocations is on the order of 0.16 μm.[8] Then, if one is interested in heterojunctions with ZnSe layers slightly below this thickness, such layers are too thin for capacitance-versus-voltage measurements. On the other hand, they are much thicker than the escape length of electrons generated at the interface, thus precluding x-ray photoelectron spectroscopy.

The band bendings of the p^+-GaAs/n^--ZnSe heterojunctions were monitored as a function of the nominal electron concentration N in ZnSe, the sample temperature T, the ZnSe thickness h, and the time elapsed since the junctions were made. From these measurements, the energy positions of the Fermi level at the junction interface with respect to the valence band of GaAs could be inferred. In dealing with GaAs one of the important questions is the ability of the bands to bend in response to heterostructure parameters or external perturbations, as opposed to the fixed band bendings usually encountered at the GaAs-air, GaAs-metal, or GaAs-insulator interfaces for a given doping level in the bulk.[9] We found that at the GaAs/ZnSe interface the band bendings in GaAs can be modified by changing the sample temperature and the nominal electron concentration in the layers. Depending on the combination of these parameters, the band bendings are larger or smaller than in the air-exposed surfaces. This means that the Fermi level at the junction interface can take positions below or above the pinning one in p-type GaAs. The values of the band bendings, in conjunction with a phenomenological model put forward to explain the experimental results, were used to extract an estimate of the band offsets. The conduction band of GaAs lies below that of ZnSe according to this estimation. In the course of the experiments, an unexpected time dependence of the band bendings with time constants on the order of several days was observed. This effect, which resembles closely the one reported for the band offsets in certain GaAs/Ge heterojunctions,[10] is attributed to instabilities of the ZnSe/GaAs interface.

The possible origin of the instabilities is discussed in light of recent findings related to ZnSe on GaAs heteroepitaxy.[11,12]

The organization of the manuscript is as follows. Section II deals with experimental details of sample preparation and Raman measurements. It includes also a description of the general characteristics of the ZnSe layers in terms of their electrical response and establishes the nomenclature to be followed in the presentation. The experimental results are described in Sec. III and their discussion is given in Sec. IV. Finally, concluding remarks are presented in Sec. V.

II. EXPERIMENT

The ZnSe layers were deposited on the (001) surfaces of GaAs substrates with bulk carrier concentration of 2×10^{19} holes/cm^3. The chemical cleaning of the GaAs surface prior to the molecular-beam deposition, the substrate temperature, and the growth rates were similar to those described previously.[1,8] The molecular beams were generated either from congruent evaporation of a polycrystalline charge of ZnSe or from elemental sources of Zn and Se operating at a relative beam pressure ratio of ≈ 1. The two approaches yielded, as expected, n^--type ZnSe layers. However, the free-electron concentration N and related transport characteristics markedly differ depending on the approach. In the films grown from the elemental sources, N is on the order of 2×10^{16} at room temperature (RT), the resistivity is about 1 Ω cm, and the mobility is typically 400 cm^2/V sec.[13] The free electrons come from the ionization of unintentionally incorporated donors present most probably in the sources. The layers produced with the polycrystalline charge have a large degree of compensation. Their resistivities at RT are in excess of 100 Ω cm and N is expected to be much smaller than the one quoted above for the other kind of layers.[13]

The transport properties of the ZnSe layers were established with Hall effect, capacitance-voltage, and current-voltage measurements performed on films thicker than 0.5 μm. The samples for Hall-effect measurements were grown on semi-insulating GaAs side by side and in the same run as those on the heavily-doped substrates. In the discussion of the Raman results, we will present detailed data on heterojunctions with the ZnSe layer thinner than 0.5 μm. For these films we will assume the same concentration of unintentionally incorporated impurities and, therefore, similar transport properties as in the thicker layers. This assumption is justified by low-temperature photoluminescence results of the ZnSe layers, which show the same features at the energies of the bound excitons and donor-acceptor–pair spectra independent of film thickness for a given method of preparing the films. The main effect of the varying thicknesses is in the position of the luminescence peaks. In the thinner films they appear renormalized to higher energies because of the built-in strain due to the lattice mismatch with the substrate. The structural properties of the interfaces were routinely checked with transmission-electron microscopy. The results for this set of samples were the same as those reported previously.[1,8] Excellent registry was found between the atomic planes of the substrates and the epilayers and misfit dislocations were absent in films thinner than 0.16 μm.

The Raman spectra were taken in the back-scattering geometry described by the notation $z(x+y,x+y)\bar{z}$ with x and y along the [100] and [010] crystallographic directions, respectively, and z parallel to the [001] growth direction. The exciting light was generated in most of the cases by an Ar^+-ion laser operating at 4880 Å and focused on the surface of the samples at a power density of about 40 W cm^{-2}. This power density provided a reasonable signal-to-noise ratio without indications of photoexcitation or heating effects. The lack of photoexcitation

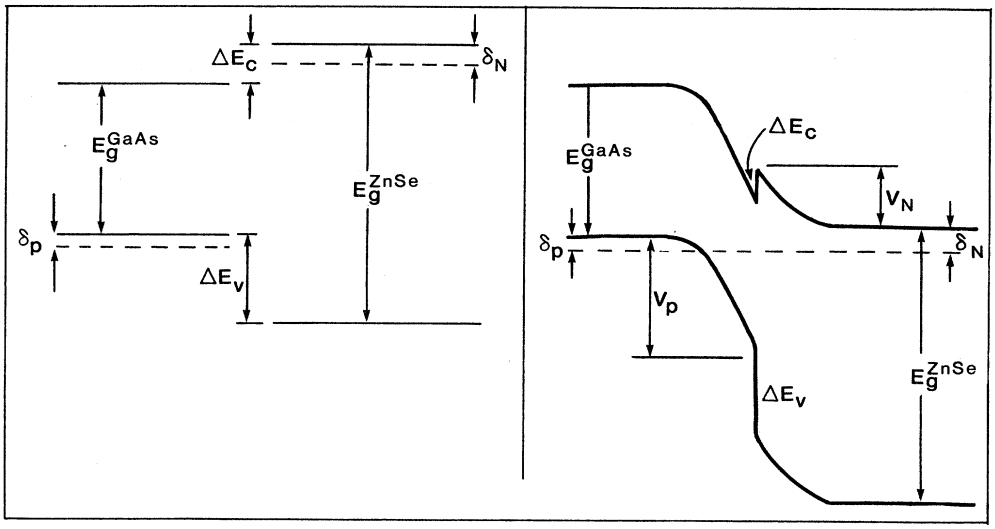

FIG. 1. Band diagram in real space before (left-hand side) and after (right-hand side) formation of the heterojunction between heavily-doped p^+-type GaAs and lightly-doped n^--type ZnSe. The drawings are for illustration purposes and for definition of the nomenclature. They are not to scale.

was checked by establishing that the Raman line shapes were independent of power densities up to ≈ 120 W cm^{-2}. The incoming photons were not absorbed in the ZnSe layers and their penetration depth in GaAs was with 300 Å on the order of the width of the space-charge layer. The Raman light was analyzed with a double monochromator and detected with photon-counting electronics.

Figure 1 illustrates general features of the band structure of the heterojunctions and defines the nomenclature that will be used throughout the paper.[7] On the left-hand side of the figure, we have the band structures of GaAs and ZnSe in real space before the junction is formed. The band gap of GaAs (E_g^{GaAs}) is ≈ 1.3 eV smaller than that of ZnSe (E_g^{ZnSe}). The Fermi level in p^+-type GaAs is measured by δ_p from the GaAs valence band and in the n^--type ZnSe by δ_N from the ZnSe conduction band. The offsets in the conduction and valence bands are represented by ΔE_c and ΔE_v, respectively. After the junction has been formed (right-hand side of the figure), the competitive processes of diffusion and drift of charges across the interface can give rise to the band bendings V_p and V_N. They, in turn, produce a built-in potential $V_D = V_p + V_N$ at the interface. In this context, it is important to mention that at the air-exposed surfaces of the GaAs substrates a fixed V_p of 0.55 eV is present. It arises because at the air/p-GaAs interface the Fermi level is strongly pinned at around 0.5±0.05 eV above the top of the valence bands,[9] and in the bulk for 2×10^{19} holes cm^{-3} δ_p lies 0.05 eV below the valence-band maximum.[7,14] The position of δ_p is independent of temperature between RT and 12 K. Typical values for the space-charge layer width and the maximum strength of the surface electric field associated with this V_p are ≈ 100 Å and 10^6 V/cm, respectively.[7] With respect to ZnSe, the large differences in N provide a broad dynamic range in the values of δ_N. For $N = 2\times 10^{16}$ electrons cm^{-3}, δ_N lies at around 20 and 170 meV below the ZnSe conduction band at 12 K and room temperature (RT), respectively. In the compensated films, the Fermi level is expected to be much further away from the conduction-band minimum and quite deep into the forbidden gap.

III. RESULTS

We discuss first the Raman results of the heterojunctions with ZnSe layers thinner than the critical layer thickness h_c; that is, the case of interfaces free of misfit dislocations.[1,8] Figure 2 shows first-order Raman spectra measured at RT and 12 K for two heterojunctions and for an air-exposed and uncoated surface of a GaAs substrate, which are included for reference purposes. Sample A has a (0.14±0.01)-μm-thick ZnSe layer and was grown from the compound source and sample B consists of a (0.12±0.01)-μm-thick ZnSe layer obtained from elemental sources. These spectra were recorded within a 12-h period after the ZnSe deposition. They are typical representatives of all the data collected for samples of

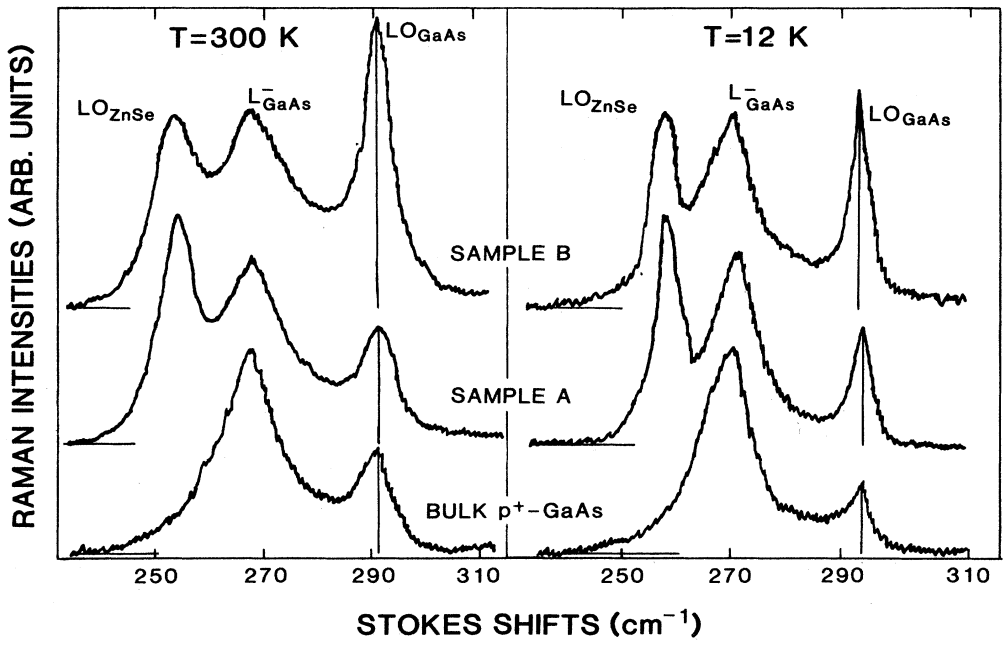

FIG. 2. First-order Raman spectra for heterojunctions A and B and a reference GaAs substrate. These line shapes were recorded within a 12-h period after the heterojunction fabrication. The spectra are normalized to the $L_{\bar{\mathrm{GaAs}}}$ intensity, and the horizontal lines indicate the background levels. The vertical lines at the $\mathrm{LO_{GaAs}}$ frequencies can be used to obtain, at a given temperature, the relative changes in intensity with respect to the control sample. The stronger $\mathrm{LO_{GaAs}}$ peaks in the heterojunctions indicate larger band bendings on the GaAs side than in the pinned air-exposed surfaces. The intensity changes are more pronounced in sample B, in line with the expected larger electron concentration in its ZnSe layer.

type A (compound source) or type B (elemental sources) and layer thicknesses $h \leq h_c$. The peaks labeled LO_{GaAs} and L^{-}_{GaAs} correspond to scattering by vibrational modes in the GaAs side of the junction. The L^{-}_{GaAs} structure is due to the hole plasmon-phonon coupled mode and the LO_{GaAs} band corresponds to the longitudinal-optical phonons in the space-charge layer. The peak frequencies at RT are 269 and 292 cm^{-1} for L^{-}_{GaAs} and LO_{GaAs}, respectively, and 271 and 295 cm^{-1} at 12 K. The LO_{ZnSe} peak arises from scattering by the longitudinal-optical phonons of the ZnSe layers of the heterojunctions. It appears at 253 and 256 cm^{-1} at RT and 12 K, respectively. The Raman modes discussed above are allowed by the scattering selection rules.[15] In the GaAs Raman peaks, the dominant scattering processes are the deformation potential mechanism for the L^{-}_{GaAs} mode and the electric-field-induced scattering for the LO_{GaAs} mode. The electric field is the one in the space-charge layer due to V_p. The deformation potential and the electro-optical mechanisms are the main scattering processes for the LO_{ZnSe} mode. However, we will see later that electric-field-induced scattering plays also a role in the Raman process of this mode. In what follows, we will be interested in the behavior of the intensities of the LO modes because of their relationship with the built-in fields. The L^{-}_{GaAs} mode has the character of a transverse-optical phonon. Its strength is not affected by changes in surface electric fields and provides for an internal calibration of intensities. We note that the reference intensity ratio LO_{GaAs}/L^{-}_{GaAs} for the p^{+}-type substrate is larger at RT than at 12 K because of the detuning of the E_1 resonance at low temperature with respect to the energy of the incoming photons. Therefore, we will compare only the LO_{GaAs} intensities of the heterojunctions with those of the reference substrate which were measured at the same temperature.

In the spectra shown in Fig. 2 one can readily see that the LO_{GaAs} intensities are stronger for the heterojunction samples than for the substrate. The length of the vertical lines at the LO_{GaAs} peaks illustrate this fact. The most dramatic increases are observed for sample B. We recall that this heterojunction corresponds nominally to the situation of a more conducting ZnSe layer with larger N and δ_N closer to the ZnSe conduction band. When compared with the reference GaAs surface, the LO_{GaAs} intensity has increased in sample B by a factor of 3.3 at 12 K and 2.8 at RT. In sample A these factors are 1.8 and 1.1 at 12 K and RT, respectively. On the other hand, no behavioral feature singles out for the LO_{ZnSe} peaks. Their intensities in the spectra of Fig. 2 correlate with the thickness of the epitaxial layers. In sample A this intensity is $\approx 20\%$ higher than in sample B. We have also measured the same absolute values of intensities for this mode in ZnSe layers with the thicknesses of samples A and B but grown on semi-insulating GaAs substrates. It appears then from these comparisons that the heterojunction formation has not affected the LO_{ZnSe} intensity within the time period mentioned above.

Following these initial measurements, the intensities of the LO peaks were monitored again after several days. Something very intriguing was then detected. The LO_{GaAs} intensity had decreased and the LO_{ZnSe} intensity had increased. The spectra drawn in Fig. 3 display the effect and give the final relationship of intensities. In this figure we are comparing the spectra obtained immediately after the heterojunctions were grown, such as those in Fig. 2 (solid line), with the data gathered several days afterwards (dashed line) when a steady-state situation was reached. The vertical arrows point out the magnitude of the changes and single out another experimental finding, namely, that the LO_{ZnSe} peaks have roughly gained in

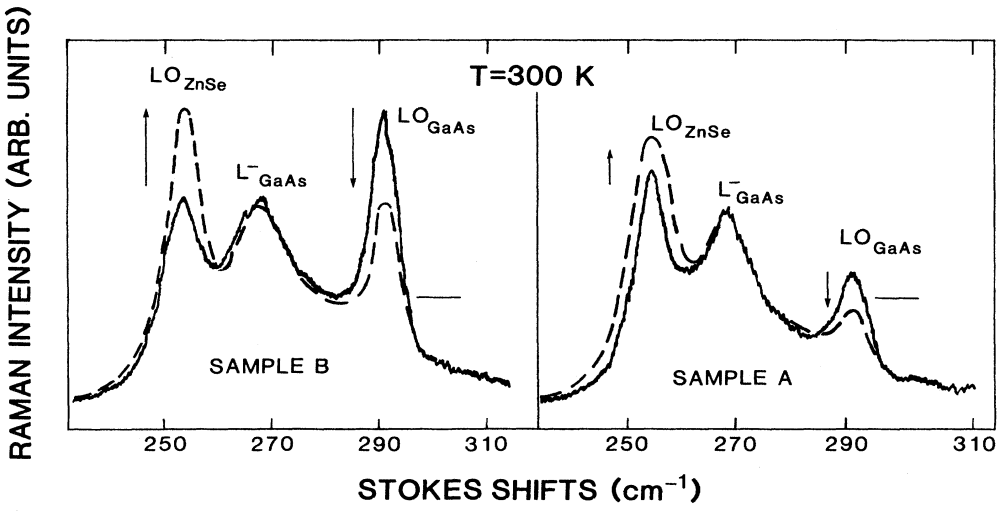

FIG. 3. Comparison between the Raman spectra of samples A and B which were taken immediately after the heterojunction formation (solid line) and several days afterwards (dashed line). The arrows render visually the interplay between the LO_{GaAs} and LO_{ZnSe} intensities. The horizontal lines give the reference values for the substrate samples. The increase in the LO_{ZnSe} intensity is taken as an indication of band-bending formation in the ZnSe layers. Note that the final LO_{GaAs} intensity in sample A is weaker than in the air-exposed surfaces. The changes of the peak intensities with time reflect some instabilities of the GaAs/ZnSe interface.

strength what the LO_{GaAs} ones have lost. The magnitude of the effect is more pronounced in sample *B*, to the extent that its LO_{ZnSe} peak appears now stronger than that in sample *A*, despite the fact that sample *B* has a thinner ZnSe layer. The horizontal lines indicate the measured intensities of the LO_{GaAs} peak in the p^+-type substrate. One can see that the final intensity of this peak in the dashed-line spectrum of sample *A* is below the reference intensity. The new ratio of intensities between the LO_{GaAs} peaks of the heterojunctions and the bulk sample are, for heterojunction *B*, 1.76 and 2.36 at RT and 12 K, respectively. For sample *A*, the ratio is 0.8 at RT and 1.5 at 12 K. At the present time we lack sufficient experimental data to correlate the temporal evolution of intensities or the rate of change with any particular set of growth conditions. However, in the case of samples of type *A*, we have compared the situations in which the final thermal cleaning of the GaAs surfaces in the growth chamber was done with and without an overpressure of As. No differences were found between these two procedures.

The variations of the LO_{GaAs} intensities in the heterostructure spectra establish that the strength of the electric field in the space-charge layer of GaAs has changed as compared with the situation in the air-exposed surfaces of the substrate.[15] These changes come about because of modifications in the band bendings V_p. The electric-field-induced contribution to the LO intensities is in first order linearly proportional to the magnitude of the band bendings.[15] Such a relationship together with a reference LO_{GaAs} intensity for the V_p in the air-exposed surfaces of the substrate can be exploited to obtain values of V_p in the heterostructures. However, one has to rule out first possible deviations from linearity that may arise when the skin depth of the Raman light and the width of the space-charge layer are comparable. We investigated this aspect experimentally by performing additional measurements in samples *A* and *B* with laser light excitation at 4131 and 4067 Å. The skin depth of the Raman light generated by these photons is on the order of 30 Å and therefore smaller than the width of the space-charge layer. We obtained with these laser lines values for the ratio of intensities which are within ±5% from those measured with the 4880-Å excitation. We infer from the comparison that absorption effects do not influence the response of the LO_{GaAs} intensities. We have not made more use of the shorter-wavelength photons because they are strongly absorbed in the ZnSe layers, thus precluding measurements in heterojunctions with ZnSe layers thicker than those in samples *A* and *B*. Additional experimental support for the applicability of the linear relationship is provided by the excellent quantitative agreement which was obtained for n^+-GaAs/n^--ZnSe heterojunctions with ZnSe layers thicker than 0.5 μm between the band bendings determined with Raman-scattering and capacitance-versus-voltage measurements.[1,16] We have then estimated V_p from the measured LO_{GaAs} intensity ratios in the heterojunction samples by calibrating the LO_{GaAs} intensity of the bulk spectra against $V_p \approx 0.55$ eV. Table I summarizes the values of V_p determined for samples *A* and *B*

TABLE I. Band bendings at room and low temperature for heterojunctions *A* and *B*. The first entry corresponds to the values immediately after the heterojunction formation and the second one after the temporal evolution. These values were obtained with a reference V_p of 0.55±0.05 eV for the air-exposed GaAs surface.

Sample	V_p (eV) 12 K	V_p (eV) 300 K	V_N (eV) 12 K	V_N (eV) 300 K
A	0.99	0.6	0	0
	0.83	0.44	0.16	0.16
B	1.83	1.54	0	0
	1.3	0.96	0.53	0.58

with the data of Figs. 1 and 2. The first entry line corresponds to V_p immediately after formation of the junctions. The second one gives the values for the steady-state situation.

We have also investigated the band bendings in heterojunctions with ZnSe layers thicker than h_c. Figure 4 displays the dependence of V_p obtained for samples grown with the polycrystalline source (type *A*). With increasing layer thickness h above h_c, V_p tends to the "pinned" value of 0.55 eV and the magnitude of the spread between the initial values of V_p (triangles) and the steady-state ones (circles) becomes less pronounced. Concomitant with these observations, the changes in LO_{ZnSe}

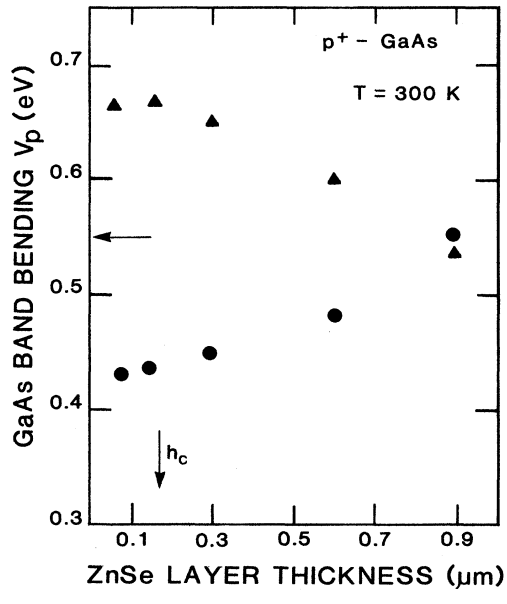

FIG. 4. Band bendings in GaAs as a function of the ZnSe layer thickness. The triangles correspond to the initial values and the circles are those after the temporal evolution. With increasing layer thickness, the band bendings approach the value for the air-exposed surface, which is singled out by the horizontal arrow. The critical layer thickness is indicated by h_c.

intensities clearly seen in Fig. 3 disappear in thicker films. Similar trends were realized in samples of type B. For clarity of the display, these data are not included in Fig. 4. As an example, we mention that for a 0.5-μm-thick ZnSe layer grown from elemental sources V_p at RT was 1 eV immediately after the growth and 0.7 eV after the steady state was reached. These values are smaller than those of heterojunction B in Table I for $h \leq h_c$, but larger than the ones of a type-A sample of comparable h in Fig. 4.

IV. DISCUSSION

The values of V_p quoted in Table I and plotted in Fig. 4 show that in the heterojunctions the band bendings can be larger or smaller than in the air-exposed GaAs surfaces. It follows, then, that the Fermi level on the GaAs side of the junction can be found in a range of energies spanning more than 1.5 eV and can take positions above or below the pinning one of 0.5 eV. In a previous study we established that ZnSe layers reduce the barrier heights at the surface of heavily-doped n-type GaAs.[1] It could have been argued at the time that this reduction comes about because the Fermi level is being repinned closer to the conduction band of GaAs and that the new pinning position is something intrinsic to the GaAs/ZnSe interface. The present results establish first that this is not the case and, second, that the band bendings in GaAs depend on the electrical nature of the ZnSe layers and on sample temperature. When the ZnSe layers are expected to be more conductive, larger values of V_p are always measured provided that h is less than 0.7 μm. For a given heterostructure with h in the neighborhood of h_c, the RT values of V_p are smaller than those at 12 K.

The ability of V_p to react to these parameters is hindered in the heterojunctions with the thicker ZnSe layers as it is shown in Fig. 4. This is because of the repinning of the Fermi level induced by the misfit dislocations. For $h \geq h_c$ misfit dislocations appear at the interface to relax the biaxial strain due to the lattice mismatch. The misfit dislocations generate interface states whose density is negligible for $h \leq h_c$ and increases continuously with h from low 10^{11} cm^{-2} for $h \approx h_c$ to mid 10^{12} cm^{-2} for $h \approx 1$ μm.[1] These states pin the Fermi level at the interface,[17] as was established in several heterostructure systems including n^+-GaAs/n^--ZnSe.[1] The point to stress from the results in Fig. 4 is that if interface states from other sources are operative for $h \leq h_c$, their density has to be smaller than those for $h \geq h_c$ otherwise we could not have been able to observe the trends shown by V_p in Table I. We will discuss these trends in more detail after we address the implications of the changes in the LO_{ZnSe} intensities.

The stronger LO_{ZnSe} peaks in the spectra displayed in Fig. 3 reveal the presence of an additional scattering mechanism in the steady-state case. This mechanism is electric-field-induced scattering,[15] which can be traced back to the formation of a built-in electric field in the ZnSe layers due to modifications in V_N.[7] In presenting the data of Fig. 2, we indicated that the LO_{ZnSe} intensities behaved quite normally when the measurements were performed immediately after the junction formation. These observations lead us to conclude that if an electric field is present in the ZnSe layers, its strength is less than 10^4 V/cm, which is a typical lower limit of electric-field strength required to induce scattering.[15] It follows from this conclusion that V_N is negligible within the initial 12-h period. This situation in which the band bendings are taken only by V_p is not stable and with time a decrease in V_p and the creation of a finite V_N in ZnSe is realized. The weaker LO_{GaAs} Raman peaks concomitant with the stronger LO_{ZnSe} ones in Fig. 3 reveal the effect. The interplay between the LO_{GaAs} and LO_{ZnSe} intensities is an indication of V_N occurring at the junction interface and not at the ZnSe-air interface. For the electric-field-induced component of the LO_{ZnSe} peak, we lack a reference calibration point. Therefore, a direct quantitative determination of V_N is not possible as it was done with V_p. However, because of the measured conservation of LO intensities and in the absence of externally applied fields the expected preservation of V_D we tentatively assign to V_N the changes measured in V_p between the initial and steady states. The so-determined values of V_N for samples A and B are given in Table I. The formation of V_N comes about because of charge depletion in the ZnSe layers. The depletion width in a ZnSe space-charge layer with a net donor density of about 2×10^{16} cm^{-3}, the quoted V_N for sample B in Table I and no potential drop at the ZnSe air interface is ≈ 0.16 μm. The magnitude of this value is comparable to the layer thickness and establishes that the assigned V_N to sample B is roughly the needed one to deplete the free electron concentration in the ZnSe layer. The smaller V_N in sample A is in line with the more compensated nature of its ZnSe layer.

The apparent initial lack of band bending in ZnSe indicates that there are no spatial differences in the energy positions of the Fermi level with respect to the conduction band between regions of the layers closer to the interface and the bulk. We mentioned before that no substantial density of interface states affects V_p for $h \leq h_c$ or the way in which it responds to the different characteristics of ZnSe and sample temperature. Based on these conclusions, we postulate that right after the formation of the junctions, V_p corresponds to the difference between the Fermi energies on both sides of the interface.[7] If the origin of energies is placed at the top of the GaAs valence band in the bulk and positive energies are measured upwards in the left-hand side part of Fig. 1, V_p can be expressed as

$$V_p = E_g^{\mathrm{GaAs}} + \Delta E_c - \delta_N - \delta_p \ . \tag{1}$$

With this convention, δ_p is -0.05 eV (independent of T), δ_N is still being measured from the conduction band of ZnSe, and ΔE_c is positive if the conduction-band edge of GaAs is below the ZnSe one. We will show that this relationship for V_p describes empirically the trends in Table I. It yields also estimates for ΔE_c which are in good agreement with previous determinations by other techniques. The dependence of V_p on T can be illustrated with sample B between 12 K and RT. The measured

difference $V_p(B, 12\text{K}) - V_p(B, \text{RT})$ with the values in Table I is equal to 0.29 eV. The prediction of Eq. (1) is $E_g^{\text{GaAs}}(12\ \text{K}) - E_g^{\text{GaAs}}(\text{RT}) - \delta_N(B, 12\ \text{K}) + \delta_N(B, \text{RT}) = 0.26$ eV, with $\delta_N(B, 12\ \text{K}) = 0.02$ eV and $\delta_N(B, \text{RT}) = 0.17$ eV, and a thermal change of 0.09 eV for E_g^{GaAs} between 12 K and RT.[14] We consider differences in V_p to eliminate ΔE_c as a parameter at this stage, and in doing so we made the usual assumption that ΔE_c does not depend on T. The dependence of V_p on the electrical nature of the ZnSe layer can be illustrated by comparing the results of sample B at 12 K and sample A at RT. This compares the extreme cases of δ_N closer to the conduction band and to midgap, respectively. From Table I we get $V_p(B, 12\ \text{K}) - V_p(A, \text{RT}) = 1.23$ eV. Equation (1) predicts a value of $E_g^{\text{GaAs}}(12\ \text{K}) - E_g^{\text{GaAs}}(\text{RT}) - \delta_N(B, 12\ \text{K}) + \delta_N(A, \text{RT}) = 1.37$ eV, if we take for $\delta_N(A, \text{RT})$ the midgap value of 1.3 eV. The overall agreement between the predicted values and the measured ones is quite satisfactory. The small discrepancies are most probably due to uncertainties in the exact values of δ_N. The largest uncertainty is in $\delta_N(A, \text{RT})$ for which we adopted the midgap value as if the compensation were perfect. However, the n-type character of the ZnSe layer of these structures indicates that δ_N can lie slightly above midgap, which will suffice to improve the agreement.

The correlations given by Eq. (1) can be exploited to extract from the measured values of V_p an estimate of ΔE_c. The most reliable values of δ_N are for sample B and, therefore, we base the analysis on its results. With the measured $V_p(B, 12\ \text{K}) = 1.83$ eV, $\delta_N(B, 12\ \text{K}) = 0.02$ eV, and $E_g^{\text{GaAs}}(12\ \text{K}) = 1.47$ eV (taking into account the gap shrinkage due to doping),[14] Eq. (1) gives $\Delta E_c = 0.33$ eV. If we use instead $V_p(B, \text{RT}) = 1.54$ eV with $E_g^{\text{GaAs}}(\text{RT}) = 1.38$ eV and $\delta_N(B, \text{RT}) = 0.17$ eV, we obtain $\Delta E_c = 0.28$ eV. The 0.05-eV difference between the two estimates is within the uncertainty in δ_N and the accuracy in the determination of V_p in the air-exposed surface of the bulk sample, which was used as reference. We will quote the average value $\Delta E_c = 0.31 \pm 0.05$ eV as the result of this study. In the case of sample A, the lack of more precise estimates of δ_N precludes a confident determination of ΔE_c. However, we can check the internal consistency of our procedure by establishing, for example, $\delta_N(A, \text{RT})$ from the measured difference $V_p(B, 12\ \text{K}) - V_p(A, \text{RT})$, and then use it to estimate ΔE_c. Instead of the midgap value we now obtain $\delta_N(A, \text{RT}) = 1.14$ eV from which a ΔE_c of 0.31 eV follows. Our determination of ΔE_c is in good agreement with values obtained in photoelectron-spectroscopy experiments,[18] and estimates from capacitance-versus-voltage measurements performed on n^+-GaAs/n^--ZnSe heterojunctions.[16] The type of band alignment reported here, and elsewhere,[16,18,19] places the GaAs conduction-band edge below that of ZnSe. In this respect, there is a disagreement with recent conclusions put forward in Ref. 20. Compared with theoretical results, the sign and magnitude of our estimate of ΔE_c agree fairly well with the predictions of several of the so-called midgap theories,[21] and with those of self-consistent linear muffin-tin-orbital calculations.[22] It is, however, in conflict with the results of pseudopotential calculations.[23,24]

We have been able to describe phenomenologically the behavior of the band bendings and their relationships to temperature, the expected electrical nature of the ZnSe layers, and the band discontinuities. We would like to address now the time evolution observed in the spectra of Fig. 3 and also given in terms of different values of band bendings in Table I and Fig. 4. The time it takes to reach the steady state is on the order of days. A time evolution of interfacial properties with similar behavior as the one reported here has been detected in Ge/GaAs heterojunctions.[10] In this particular system, the temporal effect was ascribed to an atomic exchange between As and Ge at the interface. The exchange comes about because of As motion which takes place within two monolayers from the interface and is mediated by the presence of antiphase domain boundaries in the epitaxial layer. We will invoke motion or exchange of atoms in the neighborhood of the GaAs/ZnSe interface to account for the observed time dependence. Recent experimental studies and models of the first growth steps of ZnSe on GaAs strongly suggest that an atomic exchange between Se and As is very likely to occur within 5–10 Å from the interface.[11,12] Such an exchange will be driven by the formation of the thermodynamically more favorable Ga—Se bonds close to the interface. A manifestation of this process will be the formation of a Zn-deficient boundary region near the interface in the ZnSe layers, as was experimentally found in some cases.[11] The method followed to grow the layers for this investigation is quite standard and is known to yield high-quality films in terms of optoelectronic properties.[25] Therefore, the time evolution measured in this study singles out an instability of the interface between ZnSe and GaAs. Instabilities of the kind discussed here reflect the formation or modification of the so-called interface dipoles,[10] and can clearly lead to the accumulation of fixed charges in the neighborhood of the interface.[26] This point is relevant in the context of our experiments because there is an issue we have not alluded to so far, namely, the fulfillment of the electrostatic boundary conditions between the heavily-doped substrate and the lightly-doped layer. Deviation from stoichiometry in ZnSe regions close to the interface can provide the charge needed to fulfill the boundary conditions. Along the same lines, the states associated with the changing stoichiometry can trap free charge trying to diffuse across the interface, thus avoiding the initial depletion of the ZnSe layers. In other terms, we are suggesting that these states help the Fermi level in ZnSe in the neighborhood of the interface to remain initially at the bulk value. This interpretation is in line with the experimental reports that the energy of the Fermi level in ZnSe surfaces does not differ substantially from the values in the bulk.[27,28] Finally some comments concerning the effect of possible interface dipoles on the band offsets. If we assume two sheets of fixed charges at a density of 10^{13} cm^{-2} (comparable to the acceptor density in the space-charge layer of GaAs) separated by 5 Å, the contribution to the band offsets by this dipole is ≈ 0.1 eV.[29] This correction is cer-

tainly within the magnitude of the uncertainty of our estimate and does not affect the conclusion about the type of band alignment.

V. CONCLUSIONS

We have studied the band bendings in the anisotype p^+-GaAs/n^--ZnSe heterojunctions. In samples with pseudomorphic ZnSe layers, we have shown that the band bendings in GaAs depends on the electrical nature of the ZnSe layers and the sample temperature, in a situation that resembles low densities of interface states. Consequently, the Fermi level can be moved above or below the pinning position in air-exposed GaAs surfaces. The ability to change the band bendings and the position of the Fermi level with respect to the top of the GaAs valence bands is hampered by the presence of misfit dislocations. An experimental value of the conduction-band offset was established. It places the ZnSe conduction-band edge above that of GaAs. A temporal evolution of the band bendings on both sides of the interface was detected and attributed to atomic exchange in the neighborhood of the interface. This exchange, which reflects the reactive nature of the interface chemistry between GaAs and ZnSe, has the potential of producing fixed charges close to the interface.

We have been able to describe from a phenomenological point of view the results of our experiments. However, we acknowledge the lack of models for the microscopic processes leading to some of the observations. The results of our investigation bring new experimental elements to the active field of interfaces and heteroepitaxy between II-VI and III-V compound semiconductors. For many of such systems one has to deal with lattice mismatch between the constituent materials which immediately raises the question about the role of interface chemistry versus structural defects in the determination of heterojunction properties. The present work has shown that Raman scattering can be a valuable tool in addressing this issue and can complement very effectively conventional techniques for surface characterization.

ACKNOWLEDGMENTS

The author would like to thank D. Cammack for the growth of the samples with molecular-beam epitaxy, J. Petruzzello for the structural analysis of the interfaces with transmission electron microscopy, and T. Marshall for communicating the results of transport measurements prior to publication. Critical readings of the manuscript and helpful discussions with D. Cammack, S. Colak, T. Marshall, and K. Shahzad are gratefully acknowledged.

[1]D. J. Olego, Appl. Phys. Lett. **51**, 1422 (1987); J. Vac. Sci. Technol. B **6**, 1193 (1988).
[2]S. K. Ghandhi, S. Tyagi, and R. Venkatasubramanian, Appl. Phys. Lett. **53**, 1308 (1988).
[3]T. Niina, T. Yamaguchi, K. Yodoshi, K. Yagi, and H. Hamada, IEEE J. Quantum Electron. **QE-19**, 1021 (1983).
[4]H. Iwana, Y. Tsunekawa, M. Shimada, T. Takamura, T. Seki, and H. Ohshima, Appl. Phys. Lett. **51**, 877 (1987).
[5]G. D. Studtmann, R. L. Gunshor, L. A. Kolodziejski, M. R. Melloch, J. A. Cooper, R. F. Pierret, D. P. Munich, C. Choi, and N. Otsuka, Appl. Phys. Lett. **52**, 1249 (1988).
[6]E. T. Yu, and T. C. McGill, Appl. Phys. Lett. **53**, 60 (1988).
[7]In the notation of H. C. Casey and M. B. Panish, in *Heterostructure Lasers* (Academic, New York, 1978), the narrower–band-gap semiconductor is represented by a lower-case letter and the larger–band-gap material by an upper-case letter.
[8]J. Petruzzello, B. Greenberg, D. A. Cammack, and R. Dalby, J. Appl. Phys. **63**, 2299 (1988).
[9]N. Newman, W. E. Spicer, T. Kendelewicz, and I. Lindau, J. Vac. Sci. Technol. B **4**, 931 (1986).
[10]R. W. Grant, J. R. Waldrop, S. P. Kowalczyk, and E. A. Kraut, Surf. Sci. **168**, 498 (1986).
[11]D. W. Tu and A. Kahn, J. Vac. Sci. Technol. A **3**, 922 (1985).
[12]M. C. Tamargo, J. L. de Miguel, D. M. Hwang, and H. H. Farrell, J. Vac. Sci. Technol. B **6**, 784 (1988).
[13]T. Marshall (private communication).
[14]D. J. Olego, and M. Cardona, Phys. Rev. B **22**, 886 (1980).
[15]G. Abstreiter, M. Cardona, and A. Pinczuk, in *Light Scattering in Solids IV,* edited by M. Cardona and G. Güntherodt (Springer, Heidelberg, 1984), p. 5, and references therein.
[16]S. Colak, T. Marshall, and D. Cammack, in Proceedings of the 19th International Conference on the Physics of Semiconductors (unpublished).
[17]J. M. Woodall, G. D. Pettit, T. N. Jackson, C. Lanza, K. L. Kavanagh, and J. W. Mayer, Phys. Rev. Lett. **51**, 1783 (1983).
[18]S. P. Kowalczyk, E. A. Kraut, J. R. Waldrop, and P. W. Grant, J. Vac. Sci. Technol. **21**, 482 (1982).
[19]E. J. Bawolek and B. W. Wessels, Thin Solid Films **131**, 173 (1985).
[20]K. Mazuruk, M. Benzaquem, and D. Walsh, J. Phys. (Paris) Colloq. **48**, C5-357 (1987).
[21]See Table I of M. Cardona and N. E. Christensen, J. Vac. Sci. Technol. B **6**, 1285 (1988).
[22]N. E. Christensen, Phys. Rev. B **37**, 4528 (1988).
[23]C. G. van de Walle, and R. Martin, Phys. Rev. B **35**, 8154 (1987).
[24]J. Ihm and M. L. Cohen, Phys. Rev. B **20**, 729 (1979).
[25]J. M. DePuydt, H. Cheng, J. E. Potts, T. L. Smith, and S. K. Mohapatra, J. Appl. Phys. **62**, 4756 (1987).
[26]W. A. Harrison, E. A. Kraut, J. R. Waldrop, and R. W. Grant, Phys. Rev. B **18**, 4402 (1978).
[27]H. Hartmann, R. Mach, and B. Selle, in *Current Topics in Materials Science,* edited by E. Kaldis (North-Holland, Amsterdam, 1982), Vol. 9, p. 1.
[28]M. Vos, F. Xu, J. H. Weaver, and H. Cheng, Appl. Phys. Lett. **53**, 1530 (1988).
[29]A. Zur, T. C. McGill, and D. L. Smith, Surf. Sci. **132**, 456 (1983).